

# OPTIMIZING BEAM BRIGHTNESS AT THE CANADIAN LIGHT SOURCE

L. Dallin, T. Summers, D. Bodnarchuk, Canadian Light Source, University of Saskatchewan,  
11 Perimeter Road, Saskatoon, Saskatchewan, S7N 0X4, Canada

## Abstract

The Canadian Light Source (CLS) storage ring has been operating routinely since commissioning was completed in the spring of 2004. Since that time the storage ring parameters have been adjusted in efforts to increase the brightness of the source. This includes changes to the operating point, reducing the transverse coupling and optimizing the dispersion at the source points. Depending on the photon energy brightness and flux from the undulators are increased by reducing the beam size or reducing the emittance. This is achieved with higher tunes which both decrease the emittance and the vertical  $\beta$ -function while increasing the horizontal  $\beta$ -function. Dispersion at the undulators can be optimized to minimize the beam emittance or beam size. Vertical coupling can be adjusted to less than 0.1% by reducing both the vertical dispersion and transverse coupling or increasing the vertical tune. The performance of the IR beamlines has been enhanced by producing coherent THz radiation from short bunch lengths.

## INTRODUCTION

To increase the brightness of the CLS the optics model was reviewed to in order to bring the model in better agreement with machine measurements. Edge focusing in the gradient dipole magnets [1] was investigated.

The electron beam emittance is derived from beam size measurements made on two diagnostic beamlines, the Optical Synchrotron Radiation (OSR) diagnostic line and the Xray Synchrotron Radiation (XSR) line. Reasonable agreement with the optics model is obtained, but further refinement is required.

Short bunches were modelled by changing one lattice parameter – the dispersion in the long straight sections. These lengths were confirmed with streak camera measurements on the OSR.

## MODELING CLS

### Dipole Pole Face Rotations

The pole face rotation (PFR) angles of the gradient dipole magnets were investigated in an attempt to explain a discrepancy between the model and the machine. In the process an error in estimating the gradient was discovered. The gradient is now seen to be  $k_1=0.397 \text{ m}^{-2}$  and not 0.393 as reported in [1]. The PFR was confirmed to be correct.

A plot of the gradient vs. position along the dipole orbit is shown in figure 1. The “ears” at each end of the distribution are taken to represent the extra vertical focusing provided by the PFR at each end of the magnet. The excess gradient at each pole face is given by

$\int k_1 = 0.3/(2E)(\int B'dl - B'_{\text{centre}}L)$  where  $B'$  is the gradient shown in figure 1,  $B'_{\text{centre}}$  is the gradient at the magnet centre,  $L$  is the magnet effective length and  $E$  is the electron energy. (The factor of 2 comes from splitting the excess gradient between both ends.) By equating the focal length of the  $\int k_1$  to the focal length of a PFR the effective pole face rotation is given by  $\text{PRF}_{\text{eff}} = \arctan[-\rho k_1]$  where  $\rho$  is the magnet radius of curvature.  $\text{PRF}_{\text{eff}}$  agrees with a previous estimate of 6.0 degrees. It is considerably smaller than half the bend angle of 7.5 degrees.

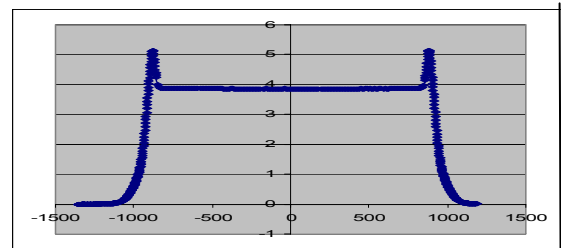


Figure 1. Dipole Gradient vs. Position

The hard edge model using this  $\text{PRF}_{\text{eff}}$  was checked by comparing the matrix elements from the hard edge model to matrix elements obtained by integrating through the actual fields and gradients. The results are shown in figure 2.

The two shallow lines are with  $\text{PRF} = 6.0$  degrees. The least error results when the fringe field integral [2] is included in the hard edge model. Slightly larger error in the vertical R43 matrix elements result when the fringe field integral is not included. The line with large errors results when the PFR is set to 7.5 degrees (or half the bend angle). Clearly, the hard edge model is a very good representation of the gradient dipole when the correct pole face rotation is used.

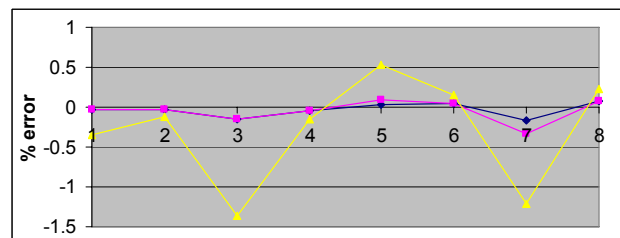


Figure 2. Errors in matrix elements of hard edge model of the gradient dipole relative to the integrating model. Position 1 is R11, 2: R12, 3: R21, 4: R22, 5: R33, 6: R34, 7: R43 and 8: R44

With the correct gradient and PFR the model for the CLS lattice is now in excellent agreement with the real machine. The model is now confidently used to estimate effects of changes in tunes and dispersion.

### Short Bunches

The symmetry of the CLS lattice allows short bunches to be produced by changing the dispersion in the centre of the long straights while holding the tunes constant as shown in figure 3. At a dispersion value of about -0.52 m the momentum compaction crosses zero. With some adjustment to the chromaticities bunch lengths less than 4 ps are predicted.

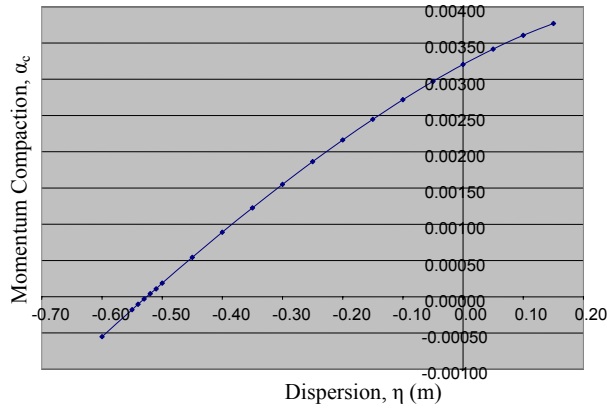


Figure 3. Momentum Compaction vs. Dispersion

### BRIGHTNESS AND FLUX

Two new storage ring setups have been compared to the present setup to see what setup will produce the highest brightness and flux for the CLS undulators. The brightness,  $B$ , is inversely proportional to the beam sizes and divergences. From [3],  $B \sim (\sigma_{Tx} \sigma_{Ty} \sigma'_{Tx} \sigma'_{Ty})^{-1}$ , where  $\sigma_T = \sigma_e^2 + \sigma_\gamma^2$ ,  $\sigma_e^2 = \beta\epsilon + (\eta\delta)^2$ ,  $\sigma_\gamma^2 = 2\lambda L / (4\pi)^2$ ,  $\sigma'_{Tx} = \sigma_e^2 + \sigma_\gamma^2$ ,  $\sigma'_{Ty} = \epsilon\gamma + (\eta'\delta)^2$  and  $\sigma'_{\gamma^2} = \lambda / (2L)$ .  $\beta$ ,  $\gamma$ ,  $\epsilon$ ,  $\eta$  and  $\delta$  are the usual electron beam parameters,  $\lambda$  is the photon wavelength and  $L$  is the total length of the undulator. In the location of the undulators  $\gamma \approx 1/\beta$  and  $\eta' = 0$ .

Also of interest is the peak angular flux density,  $dF/(d\theta d\phi)$ . This is the spectral flux divided by the beam divergences. I.e.,  $dF/(d\theta d\phi) \sim (\sigma'_{Tx} \sigma'_{Ty})^{-1}$ . Angular flux density will be called "flux" in what follows.

Table 1. Parameters for Three Machine Setups.

Parameter	Present	High tune	High dispersion
$\nu_x$	10.22	<b>11.22</b>	10.22
$\epsilon_x$ (nm-rad)	17.87	13.99	13.15
$\Delta$ (%)	0.111	0.108	0.112
$\beta_x$ (m)	9.11	15.81	8.27
$\eta_x$ (m)	0.15	0.15	<b>0.25</b>
$\nu_y$	4.28	4.28	4.28
coupling	0.002	0.002	0.002
$\epsilon_y$ (nm-rad)	0.036	0.028	0.026
$\beta_y$ (m)	2.63	2.56	2.59
$\eta_y$ (m)	0.0	0.0	0.0

The storage ring parameters for the present setup and two new setups (high tune and high dispersion) are shown in Table 1. CLS undulator parameters are shown in Table 2. From these parameters the relative beam sizes are calculated.

Table 2. CLS Undulator Parameters.

	PGM	SGM	SM	CMCF
L (m)	1.757	1.193	1.613	1.45
Energy range (keV)	0.005 - 0.25	0.25 - 1.9	0.1 - 3.0	6 - 18

The relative increase in intensity for the new setups are shown in figure 4.

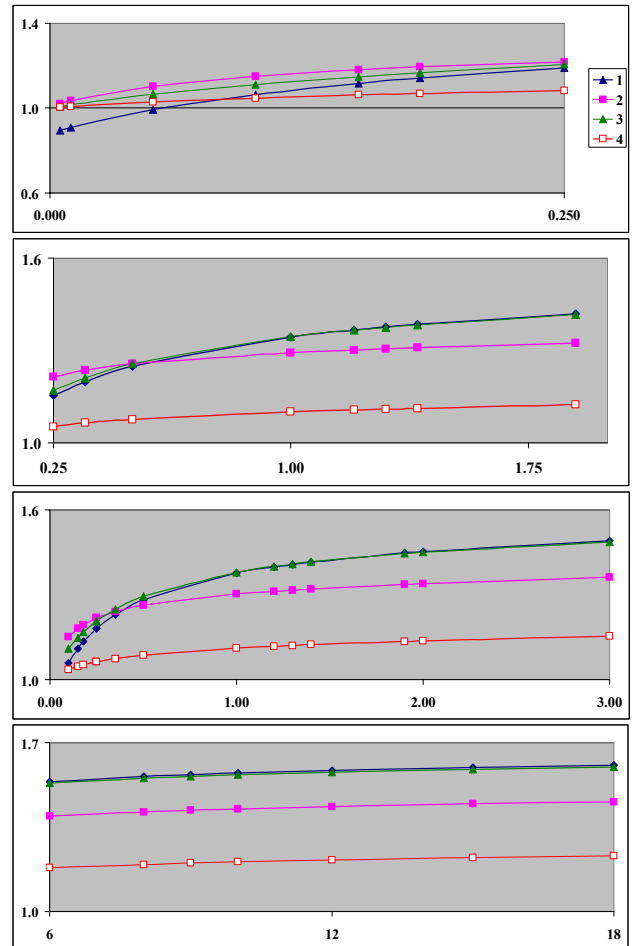


Figure 4. Increase in intensity vs. photon energy for new setups relative to the present setup. Top to bottom: PGM, SGM, SM and CMCF. 1: High tune brightness 2: High dispersion brightness 3: High tune flux 4: High dispersion flux

At low photon energies the high dispersion setup results in the best improvement as seen for the PGM undulator. For higher energy photons the high tune setup is best for increasing both brightness and flux. This is most obvious in the CMCF undulator where both brightness and flux are increased by over 50%. At this time the high

dispersion setup is available and can be used to increase brightness by over 40% at high photon energies.

The high tune setup has been achieved but more work is required to establish good injection efficiencies at this new tune. The effect on beam lifetime and beam stability also has to be studied for this mode.

## BEAM MEASUREMENTS

Since the beam sizes determine the brightness of the source an accurate measurement of the sizes is important to confirm the optics is performing as expected.

### Emittance

Beam size at the CLS are measured in two diagnostic (dipole) beamlines, the OSR[4] and the XSR[5].

The two beamlines use different techniques to extract the beam emittance. In the OSR the beam image is corrected for diffraction, depth of field, dispersion, curvature and chromatic effects to get the “true” beam size. These sizes are divided by the theoretical  $\beta$ -functions to get the horizontal and vertical emittances. In the XSR the observed beam size is compared to a Fresnel model of the beam transported through the XSR optics accounting for diffraction and geometric effects.

Results from the two beamlines give emittances in agreement within a few per cent. The best beam size measurement is obtained from the XSR. However, it gives results about 10% high for the horizontal emittance. Several possible sources of error have been investigated through tracking in the lattice model. This included the effect of the energy shift while passing through the cavity and adiabatic variation of the cavity voltage and phase. No large effect was found in these studies.

Another possible source of error is deviation of the  $\beta$  and  $\eta$ -functions at the XSR. The  $\beta$ -functions have been computed by analysing the orbit response matrices as described in [6]. An example is shown in figure 5. It appears that 10% errors in  $\beta$  are possible.

The horizontal emittances for the normal setup and the high dispersion setup have been measured to be 22.7 and 17.8 nm-rad, respectively. Although the numbers are higher than theory the high dispersion emittance is seen to be 79% of the present setup while theory predicts 74%. This suggests that the brightness increase will be close to that shown in figure 4.

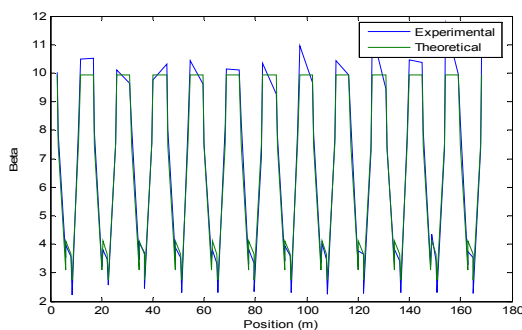


Figure 5. Horizontal  $\beta$ -functions at the position monitors and orbit correctors

### Short Bunches

In January, this year, THz radiation was observed from a single 6 mA bunch. Enhanced radiation was first observed at a dispersion of -0.45 m and continued to increase as the dispersion approached -0.52 m. The bunch length ( $1\sigma$ ) at  $\eta=-0.50$  was measured in the OSR to be less than 20 ps. At 0.25 THz the photon intensity was up to 10,000 times that of non-coherent radiation.

### Coupling Control

Transverse coupling correction at the CLS is well in hand. With the normal storage ring setup 0.1% coupling is easily achieved, 0.06% is possible with a small increase in the vertical tune. The normal operating point has been set at 0.2% as a compromise between vertical beam size and beam lifetime.

The coupling is controlled with 17 of the 36 skew quads in the ring, measurements and calculations are done with a locally written Matlab program. To correct to 0.1%, the maximum gradient in any skew quad was 0.005 m<sup>-2</sup>. It is anticipated that this will decrease as the remaining skew quads become available later this year.

The vertical tune was shifted from 4.28 to 4.468 in steps of 0.01 and the coupling was measured at each point as shown in figure 6. The skew quads were held fixed during this time.

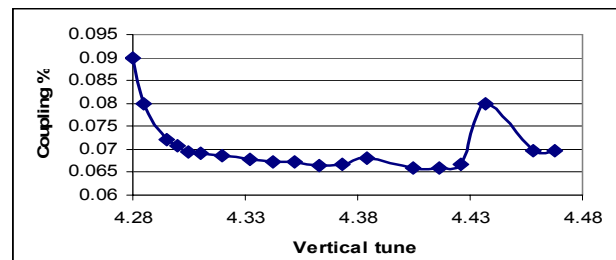


Figure 6. Variation in coupling as a function of vertical tune. The excursions are due to higher order resonances.

It is clear that a small increase in vertical tune will give a further reduction in vertical beamsizes, thus increasing brightness further.

## REFERENCES

- [1] L. Dallin et al, “Gradient Dipole Magnets for the Canadian Light Source”, EPAC 2002, p. 2340.
- [2] Karl L. Brown, SLAC report no. 75.
- [3] K.-J. Kim, “Characteristics of Synchrotron Radiation”, AIP Conference Proceedings 184, p. 567
- [4] J.C. Bergstrom, J.M. Vogt, “The Optical Diagnostic Beamline at the Canadian Light Source”, Nucl. Instr. and Methods in Phys. Research A, vol. 562, 2006, p. 495.
- [5] J.C. Bergstrom, J.M. Vogt, to be published in Nucl. Instr. and Methods.
- [6] Y. Chung, G. Decker and K. Evans, Jr., “Measurement of Beta-Function and Phase Using the Response Matrix”, PAC 1993, p. 188.